Electronic structure and dynamical properties of the periodic Anderson model

Xiaobing Feng,* Minghui Qiu, Junxia Mu, Weiguang Gao, and Aimin Shi
Department of Physics, Dalian Railway Institute, 116028 Dalian, People's Republic of China
(Received 7 September 2000; published 31 January 2001)

The density of states, dynamic magnetic susceptibility, and the dynamic electric conductivity of the periodic Anderson model have been investigated using the coherent potential approximation combining with the functional integral method. In the case of particle-hole symmetry, the density of states (DOS's) at about Fermi energy have strong temperature dependence, and there are gaps in the DOS's of the two kinds of electrons. Our theoretic results of the dynamic magnetic susceptibility and the dynamic electric conductivity are in accordance with some experiments on Kondo insulators.

DOI: 10.1103/PhysRevB.63.085101 PACS number(s): 71.27.+a, 71.10.Fd, 65.40.−b

I. INTRODUCTION

As typical strongly correlated electronic systems, heavy fermion systems (HFS's) have many anomalous properties, such as the small antiferromagnetically ordered magnetic moment,[1] non-Fermi liquid (NFL) behaviors,[2] metal-insulator transition,[3] and the microscopic coexistence of antiferromagnetism and superconductivity,[4] complex superconducting order parameter,[5] etc., apart from the extremely large electronic specific heat coefficient. It is important to study these phenomena in order to give a thorough understanding of HFS's, and it would also help us to understand the other strongly correlated electronic systems. The periodic Anderson model (PAM) and its variants [with generalization to multiconduction bands or SU(N) symmetry, etc.] have been used in most theoretical works.[6] Some conduction bands in HFS are formed by (3*d*) electrons. Apart from the degeneracy, there are also strong on-site Coulomb interactions between 3*d* electrons. The Coulomb correlation between 3*d* electrons play an important role in the Kondo insulators,[7] and the many anomalous properties of high-temperature superconductors are also caused by the strong Coulomb interaction between 3*d* electrons of Cu. Recently, a new kind of HFS without *f* electrons, LiV_2O_4,[8] has been discovered. The recent studies have shown that the correlation among conduction-band electrons has an important effect on the formation of heavy quasiparticles[9] and the non-Fermi liquid behavior.[10]

One of the most prominent characters of HFS's is the antiferromagnetic spin fluctuation (ASF). Many experiments show that the ASF plays a very important role in the formation of heavy quasiparticles and the superconducting pairing mechanism.[11] The recent study of Mathur *et al.* on $CePd_2Si_2$ and $CeIn_3$ has again shown that there are strong evidences that the ASF is responsible for the Cooper pairs formation and the NFL behavior of the resistivity above T_c.[12] The similar interaction may be responsible for the pseudogap in high-temperature superconductors.[13] In some HFS's, the Néel temperature can be driven to zero through doping or applying pressure, such as $CePd_2Si_2$, $CeNi_2Ge_2$,[14] and $CeCu_{5.9}Au_{0.1}$.[15,16] The NFL behaviors of thermodynamic and transport properties of these systems have been observed. It is also proposed that spin fluctuations may result in the NFL behaviors in some HFS's with a quantum critical point.[17–19]

In this paper, we mainly study the electronic structure and the dynamic properties of the PAM with the particle-hole symmetry. Using the method of combining functional integral and the coherent potential approximation (CPA),[20–22] the density of states (DOS) of the two kinds of carriers, the dynamic magnetic susceptibility $\chi(\omega)$, and the dynamic electric conductivity $\sigma(\omega)$ (Ref. 23) have been calculated. In the case of particle-hole symmetry, the dynamic magnetic susceptibility and the dynamic electric conductivity are qualitatively in accordance with the experiments on Kondo insulators.

II. MODEL AND FORMULAS

The periodic Anderson model reads as

$$H=\sum_{\vec{k}\sigma}\epsilon_{\vec{k}}c^{\dagger}_{\vec{k}\sigma}c_{\vec{k}\sigma}+\sum_{i\sigma}\epsilon_f f^{\dagger}_{i\sigma}f_{i\sigma}+V\sum_{i\sigma}(c^{\dagger}_{i\sigma}f_{i\sigma}+\text{H.c.})+U\sum_i n_{i\uparrow}n_{i\downarrow}, \quad (1)$$

in which $c_{\vec{k}\sigma}(c^{\dagger}_{\vec{k}\sigma})$ and $f_{i\sigma}(f^{\dagger}_{i\sigma})$ are the annihilation (creation) operators of conduction-band electrons and *f* electrons, respectively. *V*, representing the intensity of the hybridization interaction between the conduction band electrons and the nearly localized $3f$ or $4f$ electrons, is the hybridization potential. $\epsilon_{\vec{k}}$ is the dispersion relationship of the conduction band, ϵ_f the on-site energy of *f* electrons. *U* is the on-site Coulomb repulsion energy experienced by two *f* electrons with opposite spins.

In this paper, we are interested in the DOS's and the dynamic properties of the PAM. The method of combining the Hubbard-Stronovich (H-S) transformation[24] and the CPA was used in the study of itinerant magnetisms,[25,26] metal-insulator transitions (M-I),[27] etc. Hasegawa pointed out that the method, when applied to the Hubbard model, is equivalent to the self-consistent renormalization theory[28] and the one-field and the two-field decomposition method of the Coulomb correlation term give qualitatively the same results.[29] The two-field method has also been used to study the M-I transition and the dynamic electric conductivity in SmB_6.[30] For simplicity, we adopt the one-field method.

The partition function of the system may be written as

$$Z=\mathrm{Tr}\left\{e^{-\beta H_0}T_\tau \exp\left[-\int_0^\beta d\tau U\sum_i n_{i\uparrow}(\tau)n_{i\downarrow}(\tau)\right]\right\}, \quad (2)$$

in which, H_0 consists of the first three terms of Eq. (1). The last term of Eq. (1) may be rewritten as follows

$$U\sum_i n_{i\uparrow}n_{i\downarrow}=\frac{U}{2}\sum_i n_i-2U\sum_i (S_i^z)^2, \quad (3)$$

in which, $S_i^z=\frac{1}{2}\Sigma_\sigma \sigma n_{i\sigma}$, it is the spin of the f electron on site i. Using the H-S transformation[24]

$$e^{a^2}=\int_{-\infty}^{+\infty} d\xi e^{-\pi\xi^2-2a\sqrt{\pi}\xi}, \quad (4)$$

and the static approximation, the partition function can be written as

$$Z=\int \prod_i d\xi_i \exp\left(-\pi\sum_i \xi_i^2\right)\mathrm{Tr} \times\left\{\exp\left[-\beta\left(H_0'+\sum_{i\sigma} E_{i\sigma}n_{i\sigma}\right)\right]\right\}, \quad (5)$$

$$H_0'=\sum_{k\sigma} \epsilon_{\vec{k}}c_{k\sigma}^\dagger c_{\vec{k}\sigma}+\sum_{i\sigma} =\overline{\epsilon}_f f_{i\sigma}^\dagger f_{i\sigma}+V\sum_{i\sigma}(c_{i\sigma}^\dagger f_{i\sigma}+\mathrm{H.c.}), \quad (6)$$

in which, $=\overline{\epsilon}_f=\epsilon_f+U/2$, $E_{i\sigma}=\sigma\sqrt{2\pi U/\beta}\xi_i$. ξ_i is a time dependent fluctuation field introduced in the H-S transformation. Its time dependence has been ignored in the static approximation. The interaction term has been converted into a disordered term, i.e., $\Sigma_{i\sigma}E_{i\sigma}n_{i\sigma}$. It represents the charge fluctuation. This term can be handled with the CPA,[20–22] and the free energy is

$$F=-\frac{1}{\beta}\ln Z=-\frac{1}{\beta}\ln\int D\xi e^{-\beta\Psi}, \quad (7)$$

$$\Psi=\frac{\pi}{\beta}\sum_i \xi_i^2+\frac{1}{\pi}\int_{-\infty}^{+\infty} d\omega f(\omega) \times\mathrm{Im}\left\{\sum_\sigma \ln[1-(E_{i\sigma}-\Sigma_\sigma)F_\sigma]\right\}, \quad (8)$$

in which, $\Sigma_\sigma(\omega)(\sigma=\uparrow,\downarrow)$ is the coherent potential introduced in the CPA. F_σ is the lattice site Green's function of f electrons. The coherent potential Σ_σ is determined by the following equation:

$$\Sigma_\sigma(\omega)=\langle E_\sigma\rangle+[\langle E_\sigma^2\rangle-\Sigma_\sigma^2(\omega)]F_\sigma(\omega). \quad (9)$$

Any physical quantity, $X(\xi_i)$, can be calculated as follows:

$$\langle X\rangle=\frac{\int d\xi_i X(\xi_i)e^{-\beta\Psi(\xi_i)}}{\int d\xi_i e^{-\beta\Psi(\xi_i)}}. \quad (10)$$

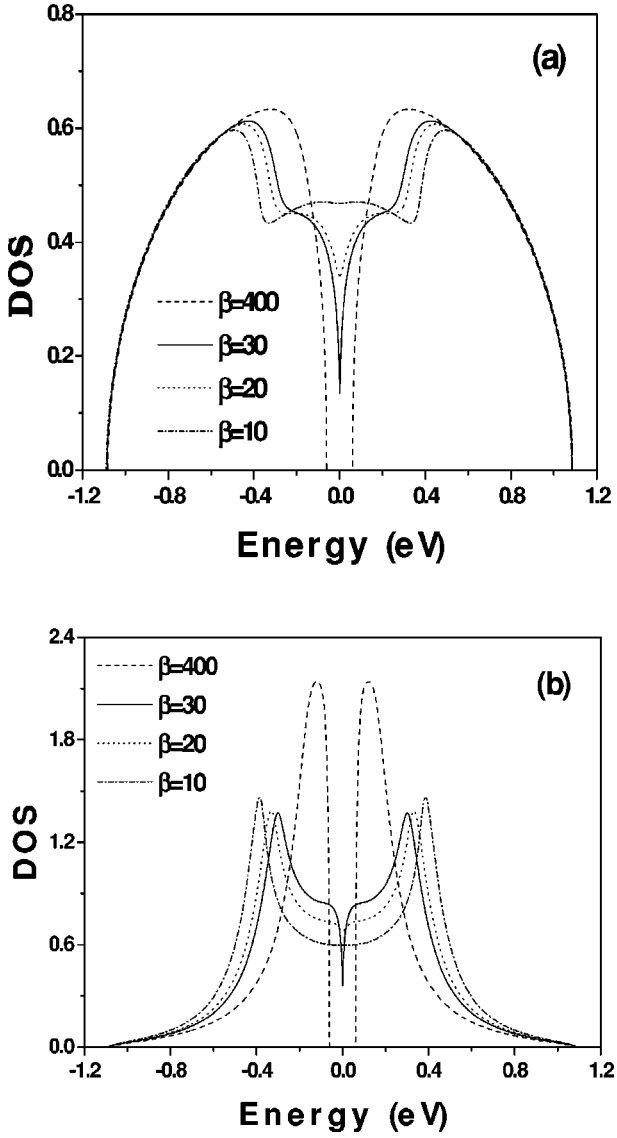

FIG. 1. The temperature dependence of the per spin per site DOS's of the conduction-band electrons (a) and the f electrons (b). The parameters are $U=0.3$, $V=0.3$, $\epsilon_f=-0.15$. $\beta=1/k_BT$ and the Fermi energy E_F is taken to be 0.

In the paramagnetic state, the f-electron lattice site Green's function reads as

$$F_\sigma(\omega)=\frac{1}{N}\sum_{\vec{k}}\frac{1}{\omega-=\epsilon_f-\Sigma_\sigma-\dfrac{V^2}{\omega-\epsilon_{\vec{k}}}}. \quad (11)$$

The average magnetic moment per site is

$$\langle m_i\rangle=-\sqrt{\frac{2\pi}{\beta U}}\langle\xi_i\rangle. \quad (12)$$

The fluctuation of the magnetic moment can be calculated as follows:

$$\langle m_i^2\rangle = \left\langle \left(-\frac{1}{\pi}\int d\omega f(\omega) \times \sum_\sigma \mathrm{Im}\left\{ \frac{\sigma F_\sigma(\omega)}{1-[E_{i\sigma}-\Sigma_\sigma(\omega)]F_\sigma(\omega)} \right\} \right)^2 \right\rangle. \quad (13)$$

In the paramagnetic state the total static magnetic susceptibility of the system consists of two parts: one from the magnetic fluctuations, and the other from H_0'. The latter can be calculated by the usual method, and the first part is given in CPA as

$$\chi = \frac{4\pi^2 U}{\beta^2}[2\pi\langle\xi^2\rangle - 1]. \quad (14)$$

In CPA, one can also calculate the dynamic properties of the system, such as the dynamic electric conductivity and dynamic magnetic susceptibility. The generalized magnetic susceptibility of any of the two kinds of electrons is defined as $\chi_{\nu\mu}(\vec{q},i\omega)=\int_0^\beta d\tau e^{i\omega\tau}\langle T_\tau M_\nu(\vec{q},\tau)M_\mu(-\vec{q},0)\rangle$, in which, $M_\nu(\vec{q})=\mu_0\Sigma_{\vec{p}ss'}\sigma^\nu_{ss'}c^\dagger_{\vec{p}+\vec{q}s}c_{\vec{p}s'}$. Here, $c_{\vec{p}s}$ represents the annihilation operator of any of the two kinds of electrons and σ^ν is the Pauli matrix. At finite temperatures the corresponding two-particle Green's function may be written as

$$\chi_{\nu\mu}(\vec{q},i\omega_n)=\frac{\mu_B^2}{V}\frac{1}{\beta}\mathrm{Tr}(\sigma^\nu\sigma^\mu)\sum_{\vec{k}m}\mathcal{G}(\vec{k},i\omega_m) \times \mathcal{G}[\vec{k}-\vec{q},i(\omega_m-\omega_n)]. \quad (15)$$

In Eq. (15), $\mathcal{G}(\vec{k},i\omega_n)$ represents the Matsubara single-particle Green's function of the conduction-band electrons or the f electrons. After the frequency summation, one can obtain the diagonal component of $\chi_{\nu\mu}$:

$$\chi(\vec{q},\omega)=-\frac{\mu_B^2}{V}\frac{1}{\pi\beta}\sum_{\vec{k}}\int d\epsilon f(\epsilon)[\mathcal{G}(-\epsilon_{\vec{k}},\epsilon+\omega+i0^+) + \mathcal{G}(-\epsilon_{\vec{k}},\epsilon-\omega-i0^+)]\mathrm{Im}\mathcal{G}(\epsilon_{\vec{k}},\epsilon+i0^+), \quad (16)$$

where $f(\omega)$ is the Fermi distribution function, $\mathcal{G}(\vec{k},\epsilon+i0^+)$ is the retarded Green's function of the corresponding Matsubara Green's function. Denoting the retarded Green's functions of the conduction band and the f electrons by $\mathcal{G}_c(\epsilon_{\vec{k}},\epsilon+i0^+)$ and $\mathcal{G}_f(\epsilon_{\vec{k}},\epsilon+i0^+)$, they have the following forms:

$$\mathcal{G}_c(\epsilon_{\vec{k}},\omega+i0^+)=\frac{1}{\omega+i0^++\mu-\epsilon_{\vec{k}}-\dfrac{V^2}{\omega+i0^++\mu-\left[\epsilon_f+\dfrac{U}{2}+\Sigma(\omega)\right]}}, \quad (17)$$

$$\mathcal{G}_f(\epsilon_{\vec{k}},\omega+i0^+)=\frac{1}{\omega+i0^++\mu-\left[\epsilon_f+\dfrac{U}{2}+\Sigma(\omega)\right]-\dfrac{V^2}{\omega+i0^++\mu-\epsilon_{\vec{k}}}}, \quad (18)$$

in which μ is the chemical potential and in this paper μ is taken to be zero. The dynamic electric conductivity $\sigma(\omega)$ can be obtained similarly. In the paramagnetic state, the system is isotropic when there is no magnetic field. The real part of the diagonal element of the $\sigma_{\mu\nu}$ is[30]

$$\sigma_1(\omega)=\frac{2Ne^2}{\pi V}\sum_\sigma\int_{-\infty}^{+\infty}d\epsilon'\frac{1}{\omega}[f(\epsilon')-f(\epsilon'+\omega)]\int_{-\infty}^{+\infty}d\epsilon A(\epsilon)\mathrm{Im}\mathcal{G}_c(\epsilon,\epsilon'+\omega+i0^+)\mathrm{Im}\mathcal{G}_c(\epsilon,\epsilon'+i0^+), \quad (19)$$

in which, $A(\epsilon)=8\pi/3\alpha(1-\epsilon^2)^{3/2}$.

III. RESULTS AND DISCUSSION

A. The density of states

On obtaining $\Sigma_\sigma(\omega)$, the DOS's of the two kinds of electrons can be calculated from the corresponding Green's functions. The DOS per site, per spin of the conduction band without hybridization is taken as[30]

$$\rho(\omega)=\begin{cases}\dfrac{2}{\pi D}\sqrt{1-\left(\dfrac{\epsilon}{D}\right)^2}, & -D\leqslant\epsilon\leqslant D\\ 0, & \text{others,}\end{cases}$$

in which D is the half width of the conduction band without hybridization, and it plays the role of an energy scale. In the following, $D=1$ is assumed.

In this paper, we concentrate mainly on the properties of PAM with the particle-hole symmetry, and the nonsymmetric case is only slightly mentioned in the following. Figs. 1(a) and 1(b) give the DOS's of conduction-band electrons and the f electrons in the paramagnetic state, respectively. It is shown that the DOS's of the two kinds of electrons have strong temperature dependence. At low temperatures there are significant gaps in the spectrums. With increasing temperature the gaps turned into pseudogaps, and finally the

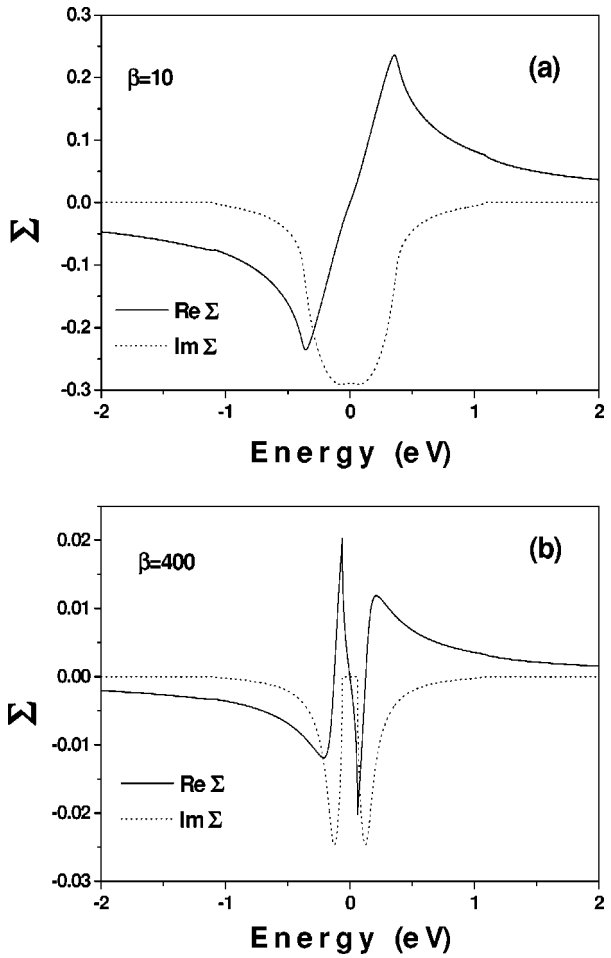

FIG. 2. The real and imaginary parts of the coherent self-energies at different temperature, $\beta=10$ in (a) and $\beta=400$ in (b).

DOS's at the Fermi energy became flat. Because of the strong temperature dependence of DOS's, the thermodynamic properties will have a strong temperature dependence, as well. The temperature dependence results from the temperature dependence of the coherent potential self-energy $\Sigma(\omega)$. The variation of $\Sigma(\omega)$ with temperature is shown in Figs. 2(a) and 2(b). The gaps in the DOS's are the reflection of the gap in the $\Sigma(\omega)$ at low temperatures.

The $\Psi(\omega)$ is given in Fig. 3. $\Psi(\omega)$ has only one minimum meaning that the system is in a paramagnetic state. With decreasing temperature, the curves of $\Psi(\omega)$ became more flat. The spin fluctuations become stronger at low temperatures. We have also calculated the DOS's in the nonsymmetric case, see Fig. 4. Under the parameters, the DOS's also have gaps. This gap also results directly from the gap in the $\Sigma(\omega)$ in Fig. 5. In this case, the thermodynamic properties are not as strongly affected by the DOS as in the symmetric case, because of the large interval between the gaps and the Fermi energy.

B. Dynamic magnetic susceptibility

Experiments show that the antiferromagnetic spin fluctuations play a very important role in the formation of heavy

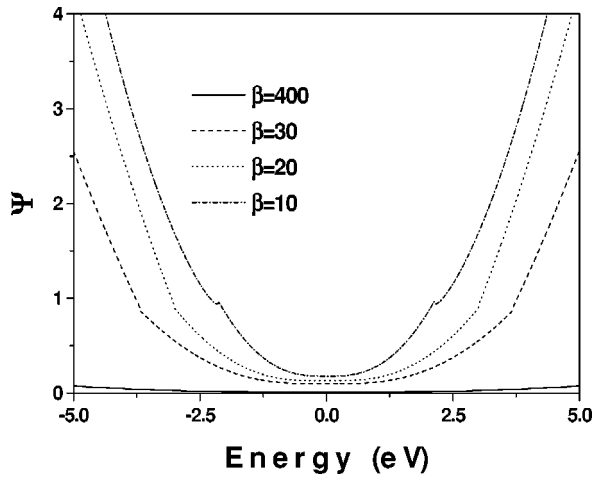

FIG. 3. The variation of $\Psi(\omega)$ with temperature.

quasiparticle and the superconductivity, as well as the many anomalous properties. Using Eq. (16) the dynamic magnetic susceptibility with wave vector dependence has been studied.

Figures 6(a) and 6(b) give the temperature dependence of real and imaginary parts of the dynamic magnetic susceptibility, $\chi_f(\omega)$, of the f electrons, with wave vector the antiferromagnetic vector $\mathbf{Q}[=(\pi,\pi,\pi)]$. At low energies, the Re χ_f increases with decreasing temperature, meaning the enhancing of the antiferromagnetic spin fluctuations. It is also shown that with decreasing temperature there appears a spin gap in the excitation spectrum. The gap is about 0.1 eV in Fig. 6(b) and equals approximately the one in the DOS. There are spectrum weight transfers to low energy, both in Re χ_f and Im χ_f, with decreasing temperature.

The temperature dependence of the real and imaginary parts of the conduction electron dynamic magnetic susceptibility with antiferromagnetic wave vector $\mathbf{Q}$ are shown in Fig. 7. Though there is also a spin gap in the spectrum and the gap disappears on increasing temperature, the magnetic susceptibility has a weaker temperature dependence.

The dynamic magnetic susceptibility with the wave vector $\mathbf{q}=(0,0,0)$ of the two kinds of electrons are shown in Figs. 8

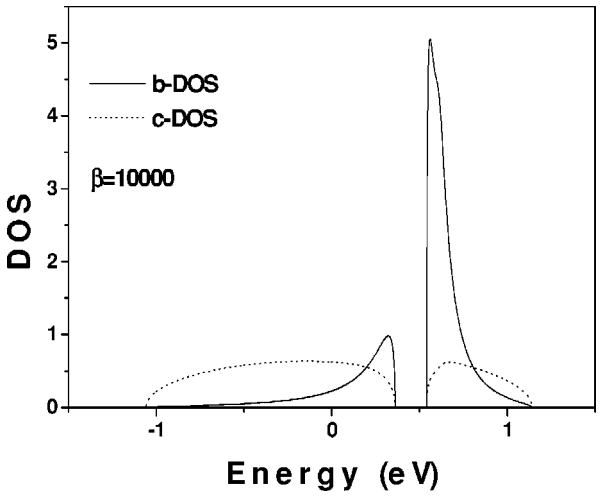

FIG. 4. The DOS's of the two kinds of electrons in the nonsymmetric case. The parameters are taken as $U=2$, $V=0.3$, $\epsilon_f=-0.5$.

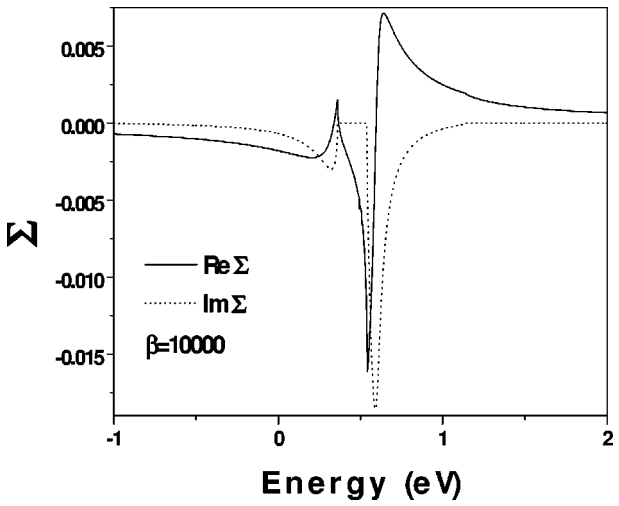

FIG. 5. The real and imaginary parts of the coherent self-energy in the nonsymmetric case.

and 9, respectively. The behaviors of the magnetic susceptibility is greatly different from the ones in the case of wave vector **Q**. The spin gaps in the spectrums are significantly larger than the gaps in the DOS's and the ones in the previous case. The gaps in the spectrums are direct gaps, while the gaps in the DOS's are indirect ones. The above results show that the direct gap with momentum transfer **Q** is nearly the same as the indirect gap, and the direct gap with no momentum transfer is much larger. Such a conclusion is in accordance with the picture of the two hybridization subbands with a hybridization gap in between. From the DOS peaks at the gap edges in Fig. 1(b), at low temperature one can know that the two subbands have a flat dispersion relationship at the origin and the edge of the first Brillouin zone, respectively.

Our results for Re $\chi(\omega)$ and Im$\chi(\omega)$ of f electrons with $\mathbf{q}=(0,0,0)$ and the Im χ with wave vector **Q** are qualitatively in accordance with the slave-boson mean field results of Riseborough.[31] As pointed out by Riseborough, these results can qualitatively account for the experimental results on $Ce_3Bi_4Pt_3$, one of the Kondo insulators.

C. Dynamic electric conductivity

In the CPA approximation, the dynamic electric conductivity can also be calculated conveniently. Figure 10 gives the temperature dependence of the real part of the dynamic electric conductivity $\sigma_1(\omega)$ in the particle-hole symmetric case. With decreasing temperature, the spectrum weight at low energies transfers to higher energy and, thus, the $\sigma_1(\omega)$ at low energies decreases monotonously. With the transfer, the system eventually became an insulator. The peak position in Fig. 10 is in accordance with the position of peaks of the magnetic susceptibility of the conduction-band electrons because in the PAM, the dynamic electric conductivity is totally contributed by the conduction-band electrons. Thus, the gap in the dynamic magnetic susceptibility of the conduction-band electrons is of the same origin as the gap in $\sigma_1(\omega)$, i.e., they result from the direct gap between energy bands.

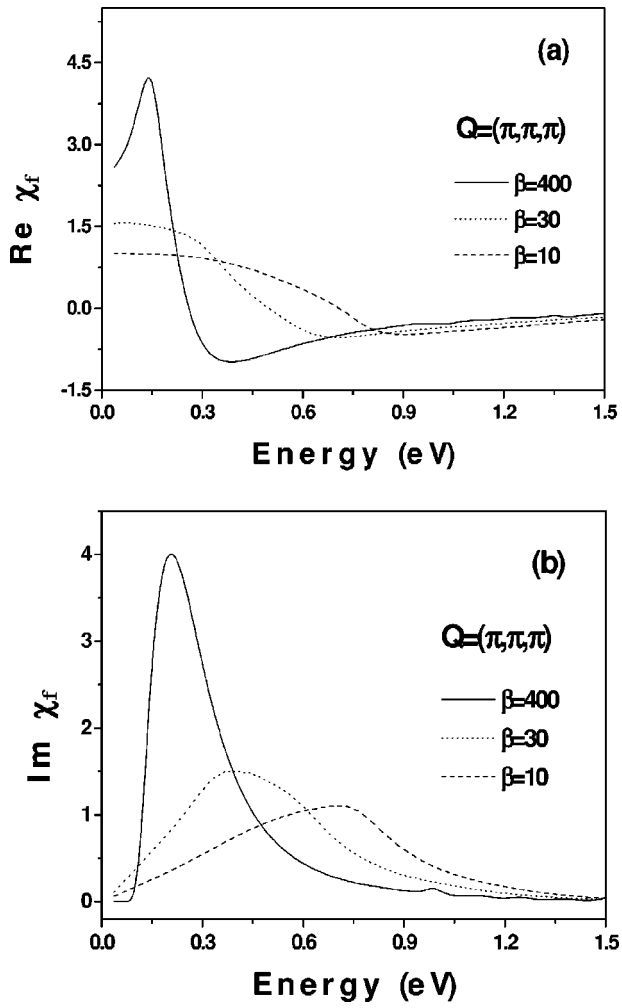

FIG. 6. The temperature dependence of the real part (a) and the imaginary part (b) of the dynamic magnetic susceptibility of the f electrons with wave vector $\mathbf{Q}=(\pi,\pi,\pi)$ in the particle-hole symmetric case.

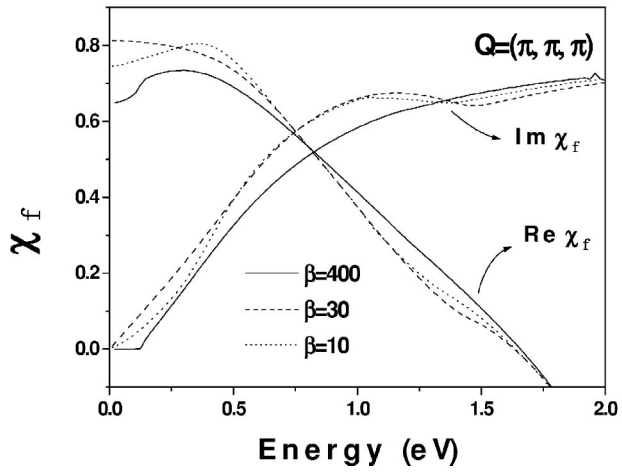

FIG. 7. The temperature dependence of the real and imaginary parts of the dynamic magnetic susceptibility of the conduction-band electrons with wave vector $\mathbf{Q}=(\pi,\pi,\pi)$.

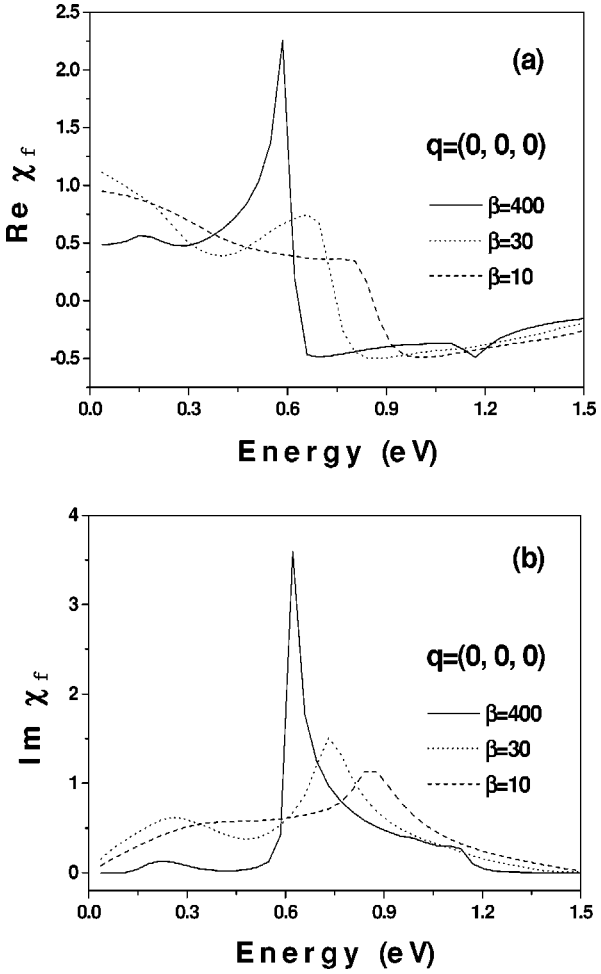

FIG. 8. The temperature dependence of the real part (a) and the imaginary part (b) of the dynamic magnetic susceptibility of the f electrons with wave vector $\mathbf{q}=(0,0,0)$.

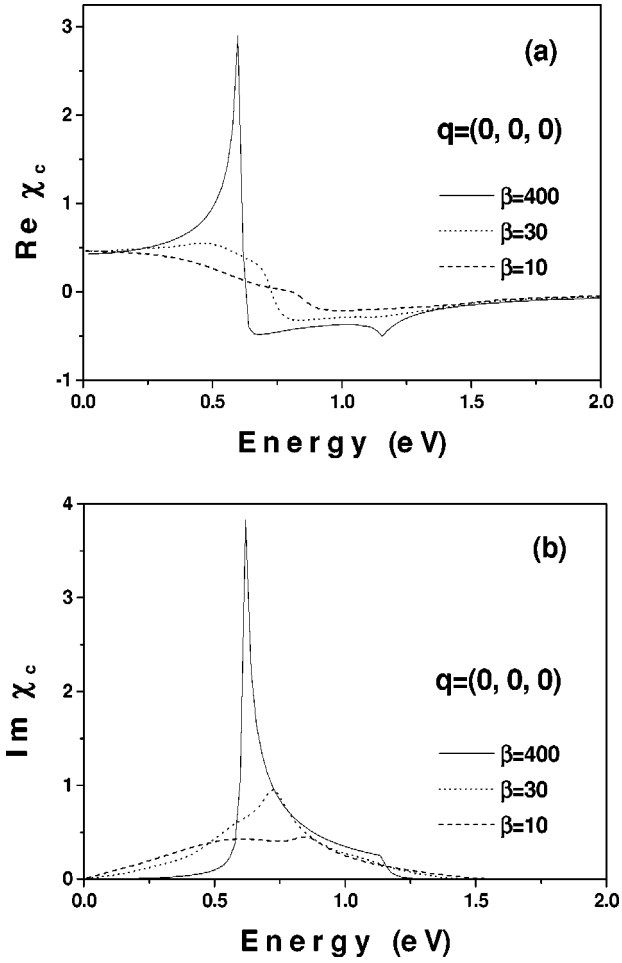

FIG. 9. The temperature dependence of the real part (a) and the imaginary part (b) of the dynamic magnetic susceptibility of the conduction-band electrons with wave vector $\mathbf{q}=(0,0,0)$.

The $\sigma_1(\omega)$ at low temperature in the nonsymmetric case is shown in Fig. 11. As the energy approaches 0, $\sigma_1(\omega)$ increases rapidly. This is the usual Drude peak. This behavior differs from that in the symmetric case. Although the DOS at the Fermi energy of conduction-band electrons shows only a small dip at $\beta=30$, there is no sign of an increase of $\sigma_1(\omega)$ at low energy. Only at higher temperature, at which the DOS became flat enough, is there an upturn of $\sigma_1(\omega)$ at low energy. The peak of $\sigma_1(\omega)$ at about 0.7 eV is equal to the energy interval between the Fermi energy and the upper band edge of the conduction-band electrons. Thus, the peak results from the single electron excitation.

The dynamic electric conductivity of some of the HFS's have been studied experimentally.[32] The $\sigma_1(\omega)$ of some of the Kondo insulators, such as $Ce_3Bi_4Pt_3$, $Fe_{1-x}Co_xSi$, SmB_6 *et al.*, increase with temperature monotonously at low frequencies, and at high frequencies the $\sigma_1(\omega)$ became temperature independent. All of these features are qualitatively in agreement with the above theoretical results. The experiment on the Kondo insulator YbB_{12} shows that the dc conductivity $\sigma(0)$ decreases monotonously with temperature, and finally, it approaches zero with decreasing temperature.[33] Such a behavior of dc conductivity is also in agreement with our results. Our results are also in accordance with the theory in Ref. 34. The experiments also show that the $\sigma_1(\omega)$ of some of the HFS's exhibiting non-Fermi liquid behaviors, such as $U_{0.2}Y_{0.8}Pd_3$, $U_{0.2}Th_{0.8}Pd_2Al_3$, and $UCu_{3.5}Pd_{1.5}$, have similar behaviors as the Kondo insulators mentioned above, though the mechanism may be quite different.[32]

IV. CONCLUSION

The DOS's of the two kinds of electrons of the PAM have been calculated. In the particle-hole symmetric case, the DOS's at the Fermi energy have a strong temperature dependence. With decreasing temperature, the DOS's at about Fermi energy develop from flat structures into pseudogaps, and finally, complete gaps. Such behaviors are in accordance with the experiments on Kondo insulators, such as YbB_{12}.[33] In correspondence with the gap in DOS, the imaginary parts of the dynamic magnetic susceptibility with wave vector $\mathbf{q}=(\pi,\pi,\pi)$ of the two kinds of electrons show spin gaps of the same size as the DOS gap. Also, the spin gaps disappear with increasing temperature. The two kinds of gaps are the reflection of the indirect gap between the two hybridization subbands. The direct gap is far larger than the direct one, and

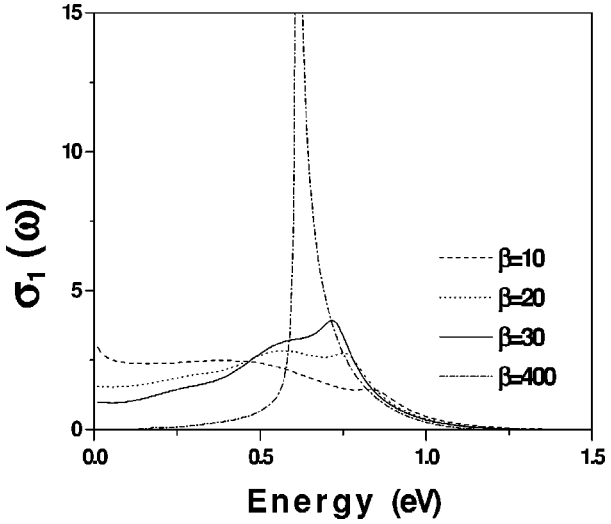

FIG. 10. The temperature dependence of the real part $\sigma_1(\omega)$ of the dynamic conductivity with particle-hole symmetry.

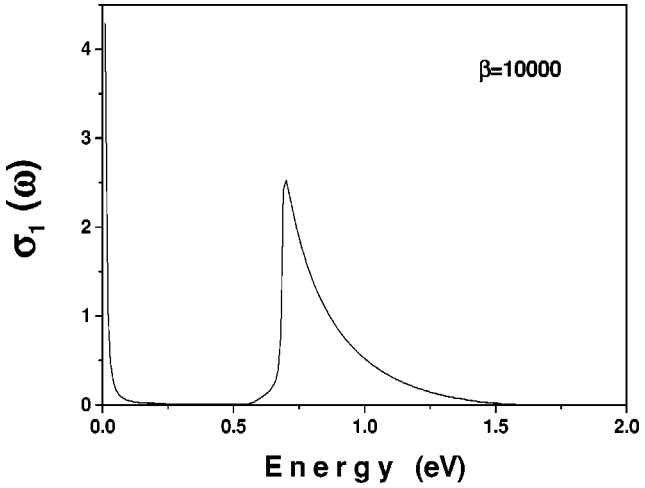

FIG. 11. The real part $\sigma_1(\omega)$ of the dynamic conductivity in the nonsymmetric case.

it is embodied in the $\mathrm{Im}\chi(\mathbf{q},\omega)$ with $\mathbf{q}=(0,0,0)$. From the temperature dependence of the $\Psi(\omega)$ and the real part of the dynamic magnetic susceptibility of the *f* electrons, one can see that the antiferromagnetic spin fluctuation became stronger with decreasing temperature. The dynamic electric conductivity shows similar behaviors as the Kondo insulators, i.e., the $\sigma_1(\omega)$ decreases monotonously with temperature at low frequencies, while at high frequencies, the $\sigma_1(\omega)$ is basically temperature independent. In the nonsymmetric case the $\sigma_1(\omega)$ differs greatly from that in the particle-hole symmetric case. There is an obvious Drude peak, nevertheless, there is only an upturn of $\sigma_1(\omega)$ at low frequencies and high temperature in the symmetric case though the DOS of the conduction-band electrons has a flat structure at the Fermi energy.

*Electronic address: xiaobingf@hotmail.com

[1] W. J. L. Buyers, Physica B **223-224**, 9 (1996).

[2] M. B. Maple, C. L. Seaman, D. A. Gajewski, Y. Dalichaouch, V. B. Barbetta, M. C. De Andrade, H. A. Mook, H. G. Lukefahr, O. O. Bernal, and D. E. MacLaughlin, J. Low Temp. Phys. **95**, 225 (1994); F. Steglich, P. Hellmann, S. Thomas, P. Gegenwart, A. Link, R. Helfrich, G. Sparn, M. Lang, C. Geibel, and W. Assmus, Physica B **237-238**, 192 (1997).

[3] G. Aeppli and Z. Fisk, Comments Condens. Matter Phys. **16**, 155 (1992); Z. Fisk, J. L. Sarrao, S. L. Cooper, P. Nyhus, G. S. Boebinger, A. Passner, and P. C. Canfield, Physica B **223-224**, 409 (1996).

[4] A. Amato, Rev. Mod. Phys. **69**, 1119 (1997); F. Steglich, P. Gegenwart, C. Geibel, R. Helfrich, P. Hellmann, M. Lang, A. Link, R. Modler, G. Sparn, N. Buttgen, and A. Loidl, Physica B **223-224**, 1 (1996).

[5] Robert H. Heffner and Michael R. Norman, Comments Condens. Matter Phys. **17**, 361 (1996).

[6] See for example, M. Lavagna, A. J. Millis, and P. A. Lee, Phys. Rev. Lett. **58**, 266 (1987); F. B. Anders, M. Jarrell, and D. L. Cox, *ibid.* **78**, 2000 (1997).

[7] M. V. Tovar Costa, A. Troper, N. A. de Oliveira, G. M. Japiassu, and M. A. Continentino, Phys. Rev. B **57**, 6943 (1998).

[8] S. Kondo, D. C. Johnston, C. A. Swenson, F. Borsa, A. V. Mahajan, L. L. Miller, T. Gu, A. I. Goldman, M. B. Maple, D. A. Gajewski, E. J. Freeman, N. R. Dilly, R. P. Dickey, J. Merrin, K. Kojima, G. M. Luke, Y. J. Uemura, O. Chmaissen, and J. D. Jorgensen, Phys. Rev. Lett. **78**, 3729 (1997); D. C. Johnston, C. A. Swenson, and S. Kondo, Phys. Rev. B **59**, 2627 (1999).

[9] Minghui Qiu, Junxia Mu, and Xiaobing Feng, Physica B **291**, 280 (2000).

[10] M. Granath and H. Johannesson, Phys. Rev. B **57**, 987 (1998).

[11] See, for example, N. Metoki, Y. Haga, Y. Koike, and Y. Onuki, Physica B **241**, 845 (1998).

[12] N. D. Mathur, F. M. Grosche, S. R. Julian, I. R. Walker, D. M. Freye, R. K. W. Haselwimmer, and G. G. Lonzarich, Nature (London) **394**, 39 (1998).

[13] Zachary Fisk and David Pines, Nature (London) **394**, 22 (1998).

[14] S. J. S. Lister, F. M. Grosche, F. V. Carter, R. K. W.Haselwimmer, S. S. Saxena, N. D. Mathur, S. R. Julian, and G. G. Lonzarich, Z. Phys. B: Condens. Matter **103**, 263 (1997).

[15] A. Schröder, G. Aeppli, and E. Bucher, Physica B **241-243**, 868 (1998).

[16] H. V. Löhneysen, F. Huster, S. Mock, A. Neubert, T. Pietrus, M. Sieck, O. Stockert, and M. Waffenschmidt, Physica B **230-232**, 550 (1997); Hilbert V. Löhneysen, Physica B **206-207**, 101 (1995).

[17] A. J. Millis, Phys. Rev. B **48**, 7183 (1993); A. J. Millis, Physica B **199-200**, 227 (1994).

[18] O. Stockert, H. V. Lohneysen, A. Rosch, N. Pyka, and M. Loewenhaupt, Phys. Rev. Lett. **80**, 5627 (1998).

[19] A. Rosch, A. Schröder, O. Stockert, and H. V. Löhneysen, Phys. Rev. Lett. **79**, 159 (1997).

[20] Fumiko Yonezawa and Kazuo Morigaki, Suppl. Prog. Theor. Phys. **53**, 1 (1973).

[21] R. J. Elliott, J. A. Krumhansl, and P. L. Leath, Rev. Mod. Phys. **46**, 465 (1974).

[22] B. Velicky, S. Kirkpatrick, and H. Ehrenreich, Phys. Rev. **175**, 747 (1968).
[23] L. Degiorgi, Rev. Mod. Phys. **71**, 687 (1999).
[24] J. Hubbard, Phys. Rev. Lett. **3**, 77 (1959).
[25] J. Hubbard, Phys. Rev. B **19**, 2626 (979); **20**, 4584 (1979).
[26] S. Q. Wang, W. E. Evenson, and J. R. Schrieffer, Phys. Rev. Lett. **23**, 92 (1969); W. E. Evenson, J. R. Schrieffer, and S. Q. Wang, J. Appl. Phys. **41**, 1199 (1970).
[27] See, for example, G. Gobsch and W. Weller, Phys. Status Solidi B **57**, 593 (1973).
[28] T. Moriya and A. Kawabata, J. Phys. Soc. Jpn. **34**, 639 (1973); T. Moriya, *Spin Fluctuations in Itinerant Electron Magnetism* (Springer-Verlag, Heidelberg, 1985).
[29] Hideo Hasegawa, J. Phys. Soc. Jpn. **46**, 1504 (1979); **49**, 963 (1980).
[30] Hideaki Ishikawa, Phys. Rev. B **28**, 5643 (1983); **28**, 5656 (1983).
[31] Peter S. Riseborough, Phys. Rev. B **45**, 13 984 (1992).
[32] L. Degiorgi, Rev. Mod. Phys. **71**, 687 (1999).
[33] T. Susaki, Y. Takeda, M. Arita, K. Mamiya, A. Fujimori, K. Shimada, H. Nmatame, M. Taniguchi, N. Shimizu, F. Iga, and T. Takabatake, Phys. Rev. Lett. **82**, 992 (1999).
[34] M. J. Rozenberg, G. Kotliar, and H. Kajueter, Phys. Rev. B **54**, 8452 (1996).